

Synchronous observation of Bell nonlocality and state-dependent Kochen-Specker contextuality

Lei Xiao,¹ G. Ruffolo,² A. Mazzari,² T. Temistocles,^{3,4} M. Terra Cunha,⁵ R. Rabelo,^{2,*} and Peng Xue^{1,†}

¹*Beijing Computational Science Research Center, Beijing 100084, China*

²*Instituto de Física “Gleb Wataghin”, Universidade Estadual de Campinas, 130830-859, Campinas, Brazil*

³*Departamento de Física, Instituto de Ciências Exatas,*

Universidade Federal de Minas Gerais, 30123-970, Belo Horizonte, Brazil

⁴*Instituto Federal de Alagoas - Campus Penedo, Rod. Eng. Joaquim Gonçalves - Dom Constantino, 57200-000, Penedo, AL, Brazil*

⁵*Instituto de Matemática, Estatística e Computação Científica,*

Universidade Estadual de Campinas, 130830-859, Campinas, Brazil

(Dated: April 14, 2022)

Bell nonlocality and Kochen-Specker contextuality are two remarkable nonclassical features of quantum theory, related to strong correlations between outcomes of measurements performed on quantum systems. Both phenomena can be witnessed by the violation of certain inequalities, the simplest and most important of which are the Clauser-Horne-Shimony-Holt (CHSH) and the Klyachko-Can-Binicioğlu-Shumovski (KCBS), for Bell nonlocality and Kochen-Specker contextuality, respectively. It has been shown that, using the most common interpretation of Bell scenarios, quantum systems cannot violate both inequalities concomitantly, thus suggesting a monogamous relation between the two phenomena. In this Letter, we show that the joint consideration of the CHSH and KCBS inequalities naturally calls for the so-called generalized Bell scenarios, which, contrary to the previous results, allows for joint violation of them. A photonic experiment thus tests the synchronous violation of both CHSH and KCBS inequalities. Our results agree with the theoretical predictions, thereby providing experimental proof of the coexistence of Bell nonlocality and Kochen-Specker contextuality in the simplest scenario, and shed new light for further explorations of nonclassical features of quantum systems.

Introduction.— Quantum theory is notable for being intriguing and counter-intuitive, a fact due, mostly, to predictions and concepts that diverge from those of classical theories. Among such nonclassical concepts are Bell nonlocality [1, 2] and Kochen-Specker contextuality [3, 4].

Classical reasoning assumes the possibility of well-defined values for every physical quantity. Probabilities are used as a consequence of partial knowledge one has regarding *the real state of affairs*. Prior to quantum theory, there was no reason to distrust such a view.

Bell nonlocality refers to stronger-than-classical correlations on outcomes of measurements performed by distant parties on composite systems. Classical reasoning allows for the possibility of the so-called *local hidden variables* (LHV) as a mathematical description of every correlation in space-like separated measurements. In a seminal paper [1], Bell showed that quantum theory admits correlations that cannot be explained by any LHV model, a result later known as *Bell’s theorem*. The *nonlocal* correlations violate inequalities that are satisfied in any LHV theory, the so-called *Bell inequalities*, the simplest and best known of which is the *Clauser-Horne-Shimony-Holt* (CHSH) inequality [5]. It is worth mentioning that Bell nonlocality in quantum systems has been extensively tested and verified in several seminal experiments [6–11].

Contextuality is a concept similar to nonlocality; in fact, it can be understood as a generalization of nonlocality that manifests also for single systems. While in classical theories, every pair of measurements can be

jointly performed, at least in principle [12], in quantum theory pairs of measurements are usually *incompatible*, preventing their joint measurability. Sets of compatible measurements are called *contexts*, and theories in which it is possible to assign values to the outcomes of measurements irrespective of the context in which they are measured are called *noncontextual hidden variable* (NCHV) theories. Kochen and Specker [4] and Bell [3] were the first to note that quantum theory admits correlations that cannot be explained by any NCHV model, a result later known as *Kochen–Specker theorem*. In 2008, Klyachko *et al.* [13] noticed that, as for nonlocality, there are inequalities that hold for all noncontextual correlations while can be violated for single quantum systems. The *Klyachko-Can-Binicioğlu-Shumovski* (KCBS) inequality became the simplest example of contextuality inequality. Interestingly, there are other contextuality inequalities that, in contrast with KCBS, can be violated by *every* quantum state [14, 15], thus revealing a property of the measurements known as *state-independent contextuality* (SIC) [16–18].

Despite their common roots related to the search for hidden variables in quantum theory, nonlocality and contextuality were developed through very distinct research programs, and it was only a few years ago that mathematical approaches to unify both concepts were proposed [19–21]. The first proposal to consider nonlocality and contextuality in the same system is due to Kurzyński, Cabello, and Kaszlikowski [22]: two parties could make

a CHSH inequality test while one of the parties would also evaluate the KCBS inequality in a subsystem, using, among others, the same incompatible measurements applied in the nonlocality test. The authors proved that in quantum theory – and in more general no-disturbing theories – there exists a trade-off relation between nonlocality and contextuality indicators, allowing for the violation of only one of these tested inequalities, and conjectured a fundamental *monogamy* relation between nonlocality and (state-dependent) contextuality. This monogamy relation was experimentally verified by Zhan *et al.* [23]; and more general monogamy relations were also identified in other scenarios [24–30]. It is worth mentioning, though, that such monogamy relations do not hold for state-independent contextuality, since the contextuality test is trivial. Recently, simultaneous observation of Bell nonlocality and state-independent Kochen-Specker contextuality was reported [31].

In the work by Kurzyński *et al.* [22], there was the implicit assumption that nonlocality tests could consider only one measurement from each party. Since, for instance, a test of the KCBS inequality demands five different measurements, each of which performed in a context with a second compatible one, each measurement used in CHSH violation could also be supplemented by a compatible one, leading to new generalized Bell inequalities, in the sense of Ref. [32].

In this Letter, we revisit the scenario considered in Ref. [22] and, by considering compatible measurements in the nonlocality test, we experimentally demonstrate that quantum systems can, actually, lead to the synchronous violation of both CHSH and KCBS inequalities. We prove, thus, that there is no fundamental monogamy relation between nonlocality and state-dependent contextuality, even in this simplest scenario where such monogamy was believed to hold. Given that both Bell nonlocality and Kochen-Specker contextuality are important resources for quantum information processing protocols, we believe that this work may be a first step in the direction of devising novel information processing tasks where both nonclassical resources can be used concomitantly.

The scenario:— Consider the following measurement scenario (its main ideas and concepts can be extended in a straightforward manner to more general scenarios): two parties, Alice and Bob, run several rounds of experiments on spatially separated laboratories, each on its respective subsystem of a composite physical system, identically prepared in every round. Let Alice be able to perform $m_A = |\mathcal{X}|$ possible measurements, labelled by $x \in \mathcal{X}$, each with $o_A = |\mathcal{A}|$ possible outcomes, labelled by $a \in \mathcal{A}$. Let Bob be able to perform $m_B = |\mathcal{Y}|$ possible measurements, labelled by $y \in \mathcal{Y}$, each with $o_B = |\mathcal{B}|$ possible outcomes, labelled by $b \in \mathcal{B}$. Assume, additionally, that some measurements of Bob are *compatible*, meaning that, in each round, Bob is able to perform sub-

sets of measurements concomitantly. Let $\mathcal{C} = \{\mathbf{y}\}$ be the set *contexts* of Bob, each element \mathbf{y} of which represents a tuple of compatible measurements. Let $\mathbf{b} \in \mathcal{B}^{|\mathcal{Y}|}$ be the (ordered) tuple of outcomes of the tuple of measurements \mathbf{y} . After sufficiently many rounds, the parties are able to estimate the following set of probabilities, the so-called *behavior* of the experiment:

$$\mathbf{p} = \left\{ p(a, \mathbf{b}|x, \mathbf{y}) \mid a \in \mathcal{A}, \mathbf{b} \in \mathcal{B}^{|\mathcal{Y}|}, x \in \mathcal{X}, \mathbf{y} \in \mathcal{C} \right\}. \quad (1)$$

Let the measurements be performed in an informationally separated way, so that the following *no-signalling conditions* hold:

$$\sum_a p(a, \mathbf{b}|x, \mathbf{y}) = p(\mathbf{b}|x, \mathbf{y}) = p(\mathbf{b}|\mathbf{y}), \quad \forall \mathbf{b}, \mathbf{y}, \quad (2a)$$

$$\sum_{\mathbf{b}} p(a, \mathbf{b}|x, \mathbf{y}) = p(a|x, \mathbf{y}) = p(a|x), \quad \forall a, x. \quad (2b)$$

Following the formalism presented in [32], we define the behavior to be *local* in this scenario, or, in other words, to admit an LHV model, if there are a variable λ , and probability distributions $p(\lambda)$, $p(a|x, \lambda)$, and $p(\mathbf{b}|\mathbf{y}, \lambda)$ such that, for all outcomes and measurements:

$$p(a, \mathbf{b}|x, \mathbf{y}) = \int p(a|x, \lambda) p(\mathbf{b}|\mathbf{y}, \lambda) p(\lambda) d\lambda. \quad (3)$$

Consider the marginal behavior of Bob’s experiment:

$$\mathbf{p}_B = \left\{ p(\mathbf{b}|\mathbf{y}) \mid \mathbf{b} \in \mathcal{B}^{|\mathcal{Y}|}, \mathbf{y} \in \mathcal{C} \right\}. \quad (4)$$

Assume it obeys the *no-disturbance* conditions:

$$\sum_{\mathbf{b}/b} p(\mathbf{b}|\mathbf{y}) = p(b|\mathbf{y}) = p(b|y), \quad \forall b, y, \quad (5)$$

where \mathbf{b}/b means that the sum is over all labels in \mathbf{b} except b . We define the marginal behavior of Bob to be *noncontextual*, or to admit an NCHV model, if there are a variable σ , and probability distributions $p(b|y, \sigma)$, and $p(\sigma)$ such that, for all outcomes of all contexts:

$$p(\mathbf{b}|\mathbf{y}) = \int \left[\prod_{y \in \mathbf{y}} p(b|y, \sigma) \right] p(\sigma) d\sigma. \quad (6)$$

With all these definitions in place, let us focus on the particular scenario we are interested in. Let Alice choose between two dichotomic measurements, $\mathcal{X} = \{0, 1\}$, $\mathcal{A} = \{-1, 1\}$ and let Bob have five dichotomic measurements, $\mathcal{Y} = \{0, 1, 2, 3, 4\}$, $\mathcal{B} = \{-1, 1\}$, available, with measurement contexts $\mathcal{C} = \{\{0, 1\}, \{1, 2\}, \{2, 3\}, \{3, 4\}, \{4, 0\}\}$. The compatibility relations between all measurements are represented in Fig. 1. The following version of the CHSH inequality holds for all behaviors that are local (according to the definition in (3)):

$$\alpha_{\text{CHSH}} = \langle A_0 B_0 \rangle + \langle A_0 B_2 B_3 \rangle + \langle A_1 B_0 \rangle - \langle A_1 B_2 B_3 \rangle \stackrel{\text{LHV}}{\leq} 2, \quad (7)$$

where

$$\langle A_x B_y \rangle = p(a = b|x, y) - p(a \neq b|x, y), \quad (8a)$$

$$\begin{aligned} \langle A_x B_y B_{y'} \rangle &= p(a = b \cdot b'|x, y, y') \\ &\quad - p(a \neq b \cdot b'|x, y, y'). \end{aligned} \quad (8b)$$

Note that, according to the definitions above, the joint measurement of $B_2 B_3$ can be regarded as a single dichotomic measurement whose outcome is given by the product $b \cdot b'$, where b and b' are the outcomes of B_2 and B_3 . The left-hand side of inequality (7) is, in essence, equivalent to the left-hand side of the standard CHSH inequality, hence the same local bound.

The marginal scenario of Bob is exactly the one considered by Klyachko and co-authors [13]. The marginal behavior \mathbf{p}_B is contextual if and only if it violates the KCBS inequality (or one of the inequalities obtained from it by relabelings of measurements and/or outcomes):

$$\begin{aligned} \beta_{\text{KCBS}} &= \langle B_0 B_1 \rangle + \langle B_1 B_2 \rangle + \langle B_2 B_3 \rangle \\ &\quad + \langle B_3 B_4 \rangle - \langle B_4 B_0 \rangle \stackrel{\text{NCHV}}{\leq} 3, \end{aligned} \quad (9)$$

where

$$\langle B_y B_{y'} \rangle = p(b = b'|y, y') - p(b \neq b'|y, y'). \quad (10)$$

The main theoretical result of this manuscript is the following:

Theorem: The CHSH inequality (7) and the KCBS inequality (9) can be concomitantly violated in quantum theory.

Proof: We give a direct proof by showing state spaces, measurements and a parameterized family of states obeying all the conditions of the scenario and leading to concomitant violations of both inequalities, for some values of the parameters. The systems of Alice and Bob are a qubit and a qutrit, respectively, whose corresponding basis states are $\{|0\rangle, |1\rangle\}$ and $\{|0\rangle, |1\rangle, |2\rangle\}$.

- (i) For Alice, choose measurement x to be given by the Pauli observables A_x :

$$A_0 = \sigma_z, \quad A_1 = \sigma_x. \quad (11)$$

- (ii) Measurement y of Bob can be represented by an observable B_y with eigenvalues in $\{\pm 1\}$ given as:

$$B_j = (-1)^j (\mathbb{1} - 2|v_j\rangle\langle v_j|), \quad (12a)$$

for $j \in \{0, 1, 2, 3, 4\}$, where $\mathbb{1}$ is the identity matrix and

$$\begin{aligned} |v_j\rangle &\propto \left[\cos\left(\frac{4\pi j}{5}\right) |0\rangle + \sin\left(\frac{4\pi j}{5}\right) |1\rangle \right. \\ &\quad \left. + \sqrt{\cos\left(\frac{\pi}{5}\right)} |2\rangle \right]. \end{aligned} \quad (12b)$$

Notice that $\langle v_j | v_{(j+1) \bmod 5} \rangle = 0$, which implies that B_j and $B_{(1+j) \bmod 5}$ commute, and, hence, are compatible.

- (iii) Consider the one-parameter family of states:

$$|\Psi(\phi)\rangle = \cos(\phi) |u\rangle + \sin(\phi) |v\rangle, \quad (13a)$$

where, for $\theta_u \sim 2.868$ and $\theta_v \sim 1.449$:

$$|u\rangle = [\cos(\theta_u) |0\rangle + \sin(\theta_u) |1\rangle] \otimes |2\rangle, \quad (13b)$$

$$|v\rangle = [\cos(\theta_v) |0\rangle + \sin(\theta_v) |1\rangle] \otimes |0\rangle. \quad (13c)$$

According to Born's rule, we have:

$$\langle A_x B_y B_{y'} \rangle = \langle \Psi(\phi) | (A_x \otimes B_y B_{y'}) | \Psi(\phi) \rangle, \quad (14a)$$

$$\langle A_x B_y \rangle = \langle \Psi(\phi) | (A_x \otimes B_y) | \Psi(\phi) \rangle. \quad (14b)$$

Any choice of $\phi \in [0.288, 0.553]$ completes the proof. \square

In the above proof, the choices of Alice are usual for the maximal CHSH violation and the choices for Bob are usual for the maximal KCBS violation. The parameters θ_u and θ_v were obtained by numerical optimization in the corresponding family, for fixed values of ϕ . Table I may help in understanding the role played by ϕ . This constructive proof allows for a natural experimental verification.

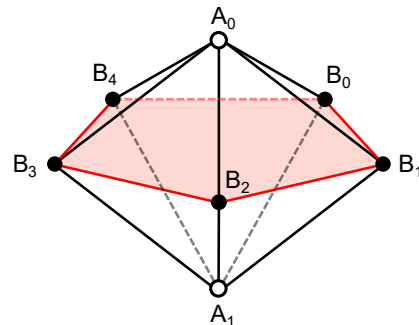


FIG. 1. Representation of the compatibility relations between all measurements in the experiment. Each measurement is represented by a vertex and vertices connected by an edge represent compatible measurements. Both measurements of Alice (white vertices) are compatible with all measurements of Bob (black vertices); compatibility of measurements of Bob is represented by a pentagon. Sets of measurements that are two-by-two compatible are jointly compatible (*e. g.*: $\{A_0, B_0, B_1\}$).

Experimental realization.— To experimentally test the concomitant violations of both KCBS and CHSH inequalities, we set up an experiment where pairs of photons were employed to encode pairs of qubit-qutrit systems. Schematics of the setup are represented in Fig. 2.

In each round of the experiment, the photons are prepared in one of the states $|\Psi(\phi)\rangle$ of the one-parameter family defined in Eq. (13). The qubit system is encoded in the polarization degree-of-freedom of one photon of the entangled pair, and the qutrit system is hybridly encoded in both the polarizations and the spatial modes of the other photon of the pair. Measurement of one of the

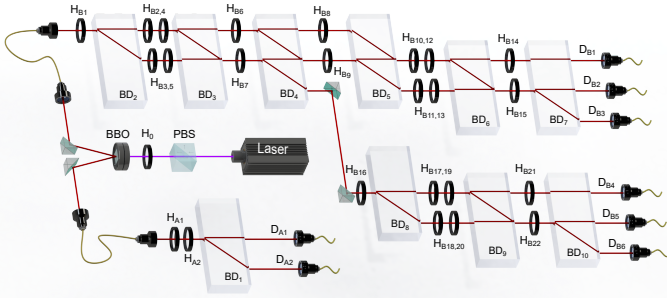


FIG. 2. Illustration of the experimental setup. Polarization-entangled photon pairs are generated via type-I spontaneous parametric down-conversion where two joint β -BBO crystals are pumped by a continuous wave diode laser. Qubit is encoded in the horizontal and vertical polarizations of one photon of each pair, while qutrit is encoded in both polarizations and spatial modes of the other photons of the entangled pairs, which are split in different paths dependent on their polarizations via a BD. For Alice, observables A_i are measured via standard polarization measurements using a HWP and a BD. For Bob, cascade Mach-Zehnder interferometers for sequentially measuring observables B_j and $B_{(j+1) \bmod 5}$ are used to test the KCBS inequality.

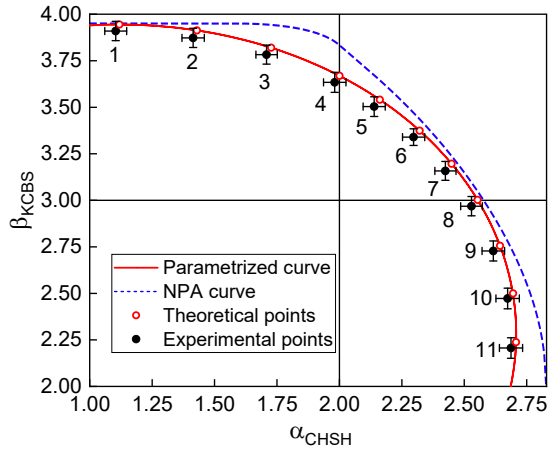


FIG. 3. Experimental results. The measurements in Eqs. (11) and (12) and the one-parameter family of states in Eq. (13) lead to the solid (red) line. Experimental data of α_{CHSH} and β_{KCBS} for specific values of the parameter ϕ are represented by the black dots and compared to their theoretical predictions (red circles). The points can be separated in three sets: points 1-4 exhibit only contextuality; points 5-7 exhibit both nonlocality and contextuality; and points 8-11 exhibit only nonlocality. Error bars are due to the statistical uncertainty in photon-number counting. Traced (blue) curve is an outer bound to the set of quantum behaviors calculated by means of the Navascués-Pironio-Acín (NPA) hierarchy [33].

observables given in Eq. (11) is, then, performed in the qubit photon, while sequential measurements of a pair of compatible observables given in Eq. (12) are performed in the qutrit photon. Details of the implementation are provided in the Supplemental Material [34].

We produce eleven points $\alpha_{\text{CHSH}} - \beta_{\text{KCBS}}$, corre-

State	ϕ (rad)	$\alpha_{\text{CHSH}}^{\text{th}}$	$\alpha_{\text{CHSH}}^{\text{exp}}$	$\beta_{\text{KCBS}}^{\text{th}}$	$\beta_{\text{KCBS}}^{\text{exp}}$
$ \Psi_1\rangle$	0	1.1188	1.1043(438)	3.9443	3.9069(518)
$ \Psi_2\rangle$	0.096	1.4293	1.4141(448)	3.9129	3.8728(514)
$ \Psi_3\rangle$	0.192	1.7269	1.7083(438)	3.8199	3.7826(510)
$ \Psi_4\rangle$	0.288	2.0005	1.9813(450)	3.6688	3.6339(536)
$ \Psi_5\rangle$	0.351	2.1622	2.1382(442)	3.5405	3.5034(529)
$ \Psi_6\rangle$	0.421	2.3215	2.2972(446)	3.3739	3.3397(446)
$ \Psi_7\rangle$	0.487	2.4495	2.4246(423)	3.1964	3.1580(506)
$ \Psi_8\rangle$	0.553	2.5536	2.5291(435)	3.0021	2.9684(517)
$ \Psi_9\rangle$	0.631	2.6433	2.6164(451)	2.7556	2.7277(537)
$ \Psi_{10}\rangle$	0.708	2.6955	2.6739(468)	2.4998	2.4726(555)
$ \Psi_{11}\rangle$	0.785	2.7075	2.6871(465)	2.2379	2.2065(553)

TABLE I. Experimental data of α_{CHSH} and β_{KCBS} for eleven input states. Error bars are due to the statistical uncertainty in photon-number counting. States 1-4 violate the KCBS inequality but not the CHSH inequality; states 5-7 violate both inequalities; and states 8-11 violate the CHSH inequality only.

sponding to eleven different input states $|\Psi_i(\phi)\rangle$ ($i = 1, \dots, 11$). The experimental results on the average values of the CHSH and KCBS operators are shown in Fig. 3 and Table I. Synchronous violation of both KCBS and CHSH inequalities are observed for the states $|\Psi_5(\phi)\rangle$, $|\Psi_6(\phi)\rangle$ and $|\Psi_7(\phi)\rangle$ with $\phi = 0.351, 0.421, 0.487$, respectively. For $|\Psi_5(\phi)\rangle$, $\alpha_{\text{CHSH}} = 2.1382 \pm 0.0442$ violates the local bound of the inequality by 3 standard deviations and is in a great agreement with the quantum prediction, 2.1622. Also, $\beta_{\text{KCBS}} = 3.5034 \pm 0.0529$ violates the noncontextual bound of the KCBS inequality by 9 standard deviations and is in great agreement with quantum prediction, 3.5405. For $|\Psi_6(\phi)\rangle$, the CHSH and KCBS inequalities are violated by 6 and 7 standard deviations, respectively. For $|\Psi_7(\phi)\rangle$, the violations are by 10 and 3 standard deviations, respectively.

To validate non-disturbance in the data and the compatibility between pairs of observables of Bob, we computed, for each state, the distance $\sum_{j=1}^5 (p_j - p'_j)^2$, where p_j is the estimated probability of outcome $b = 1$ of the observable B_j measured in one context, and p'_j is the corresponding probability of the same observable measured in the other context. As shown in Supplementary Material, the distances for all the states being tested are small enough (< 0.0005), which indicates that a very good level of non-disturbance and compatibility between observables holds in our experiment.

Conclusion and discussion.— In Ref. [22], the authors showed that the CHSH inequality and the KCBS inequality could not be violated simultaneously by quantum systems. Their proof uses a usual hypothesis for Bell scenarios, that each part makes one measurement per round. However, since one part is necessarily measuring other compatible observables in order to show contextuality, it is natural to use the locality concept of Ref. [32].

In this Letter, we show that using a more natural notion of locality, the data available in a joint test of CHSH and KCBS can produce joint violation of both inequalities, defying the concept of monogamy between contextuality and nonlocality. We provide examples of states and measurements that lead to such joint violation, and employ a photonic implementation to experimentally demonstrate, for the first time, the synchronous observation of both Bell nonlocality and state-dependent Kochen-Specker contextuality. Our experimental results agree with theoretical predictions, providing a strong evidence that these phenomena are not only non-monogamous, but may be observed and manipulated in simple quantum systems.

From the fundamental point of view, the results presented in this Letter shine new light in the relationship between two of the most important phenomena of the foundations of quantum physics. From the practical point of view, on the other hand, considering the individual importance of Bell nonlocality and Kochen-Specker contextuality to quantum information science, quantum cryptography and quantum computing, we believe that this work may lead to novel possibilities where both concepts could be jointly employed for quantum information processing protocols.

As mentioned in the introduction, there are several results on monogamy between Bell nonlocality and Kochen-Specker contextuality that use the same definition of locality as the one used by Kurzyński, Cabello, and Kaszlikowski [22]. Clearly, such results cannot be directly transposed to the more natural definition used here. Are there, however, measurement scenarios where both definitions agree on whether nonlocality and contextuality are monogamous? This is an important open question that will be investigated in the future work.

Acknowledgments:— R. R. thanks Pawel Kurzyński for fruitful discussions. This work has been supported by the National Natural Science Foundation of China (Grant Nos. 12025401, U1930402, 12088101), the Brazilian National Council for Scientific and Technological Development (CNPq) via the National Institute for Science and Technology on Quantum Information (INCT-IQ) (Grant No. 465469/2014-0), the São Paulo Research Foundation FAPESP (Grant Nos. 2018/07258-7, 2021/01502-6, 2021/10548-0).

* rabelo@ifi.unicamp.br

† gnep.eux@gmail.com

- [1] J. S. Bell, *Physics* **1**, 195 (1964).
 [2] N. Brunner, D. Cavalcanti, S. Pironio, V. Scarani, and S. Wehner *Rev. Mod. Phys.* **86**, 419 (2014).
 [3] J. S. Bell, *Rev. Mod. Phys.* **38**, 447 (1966).
 [4] S. Kochen and E. P. Specker, *J. Math. Mech.* **17**, 59 (1967).

- [5] J. F. Clauser, M. A. Horne, A. Shimony, and R. A. Holt, *Phys. Rev. Lett.* **23**, 880 (1969).
 [6] S. J. Freedman and J. F. Clauser, *Phys. Rev. Lett.* **28**, 938 (1972).
 [7] A. Aspect, J. Dalibard, and G. Roger, *Phys. Rev. Lett.* **49**, 1804 (1982).
 [8] B. Hensen, H. Bernien, A. E. Dréau, A. Reiserer, N. Kalb, M. S. Blok, J. Ruitenbergh, R. F. L. Vermeulen, R. N. Schouten, C. Abellán, W. Amaya, V. Pruneri, M. W. Mitchell, M. Markham, D. J. Twitchen, D. Elkouss, S. Wehner, T. H. Taminiau, and R. Hanson, *Nature* **526**, 682–686 (2015).
 [9] M. Giustina, M. A. M. Versteegh, S. Wengerowsky, J. Handsteiner, A. Hochrainer, K. Phelan, F. Steinlechner, J. Kofler, J.-Å. Larsson, C. Abellán, W. Amaya, V. Pruneri, M. W. Mitchell, J. Beyer, T. Gerrits, A. E. Lita, L. K. Shalm, S. W. Nam, T. Scheidl, R. Ursin, B. Wittmann, and A. Zeilinger, *Phys. Rev. Lett.* **115**, 250401 (2015).
 [10] L. K. Shalm, E. Meyer-Scott, B. G. Christensen, P. Bierhorst, M. A. Wayne, M. J. Stenvens, T. Gerrits, S. Glancy, D. R. Hamel, M. S. Allman, K. J. Coakley, S. D. Dyer, C. Hodge, A. E. Lita, V. B. Verma, C. Lambrocco, E. Tortorici, A. L. Migdall, Y. Zhang, D. R. Kumor, W. H. Farr, F. Marsili, M. D. Shaw, J. A. Stern, C. Abellán, W. Amaya, V. Pruneri, T. Jennewein, M. W. Mitchell, P. G. Kwiat, J. C. Bienfang, R. P. Mirin, E. Knill, and S. W. Nam. *Phys. Rev. Lett.* **115**, 250402 (2015).
 [11] W. Rosenfeld, D. Burchardt, R. Garthoff, K. Redeker, N. Ortiegel, M. Rau, and H. Weinfurter, *Phys. Rev. Lett.* **119**, 010402 (2017).
 [12] M. Terra Cunha, *Phil. Trans. R. Soc. A* **377**, 20190146 (2019).
 [13] A. A. Klyachko, M. A. Can, S. Binicioglu, and A. S. Shumovsky, *Phys. Rev. Lett.* **101**, 020403 (2008).
 [14] A. Cabello, *Phys. Rev. Lett.* **101**, 210401 (2008).
 [15] S. Yu and C. H. Oh, *Phys. Rev. Lett.* **108**, 030402 (2012).
 [16] N. D. Mermin, *Phys. Rev. Lett.* **65**, 3373 (1990).
 [17] A. Peres, *J. Phys. A: Math. Gen.* **24** L175 (1991).
 [18] A. Cabello, J. M. Estebarez, and G. García-Alcaine, *Phys. Lett. A* **212**, 183 (1996).
 [19] A. Cabello, S. Severini, and A. Winter, *Phys. Rev. Lett.* **112**, 040401 (2014).
 [20] A. Acín, T. Fritz, A. Leverrier, and A. B. Sainz, *Comm. Math. Phys.*, **334**, 533 (2015).
 [21] R. Rabelo, C. Duarte, A. J. López-Tarrida, M. Terra Cunha, and A. Cabello, *J. Phys. A: Math. Theor.*, **47**, 424021 (2014).
 [22] P. Kurzyński, A. Cabello, and D. Kaszlikowski, *Phys. Rev. Lett.* **112**, 100401 (2014).
 [23] X. Zhan, X. Zhang, J. Li, Y. Zhang, B. C. Sanders, and P. Xue, *Phys. Rev. Lett.* **116**, 090401 (2016).
 [24] B. Toner and F. Verstraete, [arXiv:quant-ph/0611001](https://arxiv.org/abs/quant-ph/0611001)
 [25] M. Pawłowski and Č. Brukner, *Phys. Rev. Lett.* **102**, 030403 (2009).
 [26] R. Ramanathan, A. Soeda, P. Kurzyński, and D. Kaszlikowski, *Phys. Rev. Lett.* **109** 050404 (2012).
 [27] R. Augusiak, M. Demianowicz, M. Pawłowski, J. Tura, and A. Acín, *Phys. Rev. A* **90** 052323 (2014).
 [28] R. Ramanathan and P. Horodecki, *Phys. Rev. Lett.* **113** 210403 (2014).
 [29] Z.-A. Jia, Y.-C. Wu, and G.-C. Guo, *Phys. Rev. A* **94**, 012111 (2016).
 [30] D. Saha and R. Ramanathan, *Phys. Rev. A* **95**,

- 030104(R) (2017).
- [31] X.-M. Hu, B.-H. Liu, J.-S. Chen, Y. Guo, Y.-C. Wu, Y.-F. Huang, C.-F. Li, and G.-C. Guo, *Science Bulletin* **63**, 1092 (2018).
- [32] T. Temistocles, R. Rabelo, and M. Terra Cunha, *Phys. Rev. A* **99**, 042120 (2019).
- [33] M. Navascués, S. Pironio, and A. Acín, *New J. Phys.* **10**, 073013 (2008).
- [34] See Supplemental Material for more details.
- [35] P. G. Kwiat, E. Waks, A. G. White, I. Appelbaum, and P. H. Eberhard, *Phys. Rev. A* **60**, R773 (1999).
- [36] R. Rangarajan, M. Goggin, and P. Kwiat, *Opt. Express* **17**, 18920 (2009).
- [37] E. Amselem, M. Rådmark, M. Bourennane, and A. Cabello, *Phys. Rev. Lett.* **103**, 160405 (2009).
- [38] A. Cabello, E. Amselem, K. Blanchfield, M. Bourennane, and I. Bengtsson, *Phys. Rev. A* **85**, 032108 (2012).

SUPPLEMENTAL MATERIAL FOR “SYNCHRONOUS OBSERVATION OF BELL NONLOCALITY AND STATE-DEPENDENT KOCHEN-SPECKER CONTEXTUALITY”

EXPERIMENTAL DETAILS

Our experimental setup consists of three modules: state preparation, Alice’s measurement, and Bob’s measurement.

In the state preparation module, entangled photons of 810nm wavelength are generated in a type-I spontaneous parametric down-conversion (SPDC) process where two joint 0.5mm-thick β -barium-borate (β -BBO) crystals are pumped by a CW diode laser with 230mW of power [35, 36]. The visibility of the entangled photonic state is larger than 97%.

One of the generated photons is sent to Alice for her measurement. The qubit is encoded in the polarization degree of freedom of Alice’s photon, i.e., $\{|0\rangle_A = |H\rangle, |1\rangle_A = |V\rangle\}$, where $|H\rangle$ represents the state of horizontal polarization and $|V\rangle$ represents vertical polarization.

The second photon is then split by a birefringent calcite beam displacer (BD_2) into two parallel spatial modes $|U\rangle$ (up) and $|D\rangle$ (down). Both polarization and spatial degrees of freedom of this photon are used, hybridly, to encode a qutrit, whose basis states are associated to the horizontal polarization in the upper mode, the vertical polarization in the upper mode, and the horizontal polarization in the lower mode, respectively, i.e., $\{|0\rangle_B = |UH\rangle, |1\rangle_B = |UV\rangle, |2\rangle_B = |DH\rangle\}$.

The preparation stage of the setup was designed to prepare states in the following one-parameter family:

$$|\Psi(\phi)\rangle = \cos(\phi)|u\rangle + \sin(\phi)|v\rangle, \quad (15a)$$

where, for $\theta_u \sim 2.868$ and $\theta_v \sim 1.449$:

$$|u\rangle = [\cos(\theta_u)|0\rangle + \sin(\theta_u)|1\rangle] \otimes |2\rangle, \quad (15b)$$

$$|v\rangle = [\cos(\theta_v)|0\rangle + \sin(\theta_v)|1\rangle] \otimes |0\rangle. \quad (15c)$$

The parameter ϕ can be adjusted via tuning the setting angles of the half-wave plates (HWPs, H_0 , H_{A1} and H_{B1} - H_{B3}). The angles of the HWPs for state preparation are listed in Table II.

ϕ (rad)	0	0.096	0.192	0.288	0.351	0.421	0.487	0.553	0.631	0.708	0.785
H_0 ($^\circ$)	0	2.716	5.429	8.137	9.907	11.865	13.696	15.500	17.555	19.350	20.253
H_{A1} ($^\circ$)	127.224	127.185	127.058	126.819	126.574	126.176	125.610	124.716	122.765	118.275	106.972
H_{B1} ($^\circ$)	45	44.584	44.136	43.614	43.199	42.624	41.899	40.852	38.727	34.069	22.600

TABLE II. Setting angles of HWPs for the state preparation. The angles of H_{B2} and H_{B3} are fixed at -45° and 0° , respectively, for preparing any initial state. The relation between H_{A1} and ϕ is $H_{A1} = 0.25 \arcsin(0.988 \sin 2\phi)$.

For the photon which is sent to Alice, the HWP (H_{A1}) is used in the preparation of the state $|\Psi(\phi)\rangle$ in Eq. (15). The measurement of observable A_i is a standard polarization measurement using HWP (H_{A2}) and a BD (BD_1). The HWP (H_{A2}) at 0° (22.5°) is used to map the eigenstates of the observable A_0 (A_1) corresponding to the eigenvalue $+1$ into the horizontally polarized state (and, in a complementary fashion, eigenvalue -1 into the vertically polarized state). The photons are detected at D_{A1} and D_{A2} right after BD_1 . The clicks at D_{A1} and D_{A2} correspond to outcomes -1 and 1 , respectively.

In the measurement of Bob’s observables B_j and their correlators, we use cascade Mach-Zehnder interferometers in three steps [37, 38]. Each observable B_j has two eigenvalues ± 1 , one of which is doubly degenerated. To realize

the measurement of B_j , we use four HWPs (H_{B_4} - H_{B_7}) and two BDs (BD_3 and BD_4). The angles of H_{B_4} and H_{B_7} are chosen properly – as displayed in Table III – so that the photons which are in the state $|v_j\rangle$ in Eq. (12b) of the main text corresponding to the nondegenerated eigenvalue (degenerated eigenvalues) are mapped to the horizontally (vertically) polarized mode after H_{B_7} . The HWPs H_{B_5} and H_{B_6} with fixed setting angles are used to fine tune the phase difference between two arms of interferometers. Beam displacer BD_4 separates the photons into two different spatial modes corresponding to the two outcomes.

Contexts	$H_{A_2}(\circ)$	$H_{B_4}(\circ)$	$H_{B_7}(\circ)$	$H_{B_9}(\circ)$	$H_{B_{10}}(\circ)$	$H_{B_{12,19}}(\circ)$	$H_{B_{15,22}}(\circ)$	$H_{B_{16}}(\circ)$	$H_{B_{17}}(\circ)$
B_0B_1	0	0	20.958	-60.985	45	-18	-20.985	24.015	45
B_1B_2	0	-18	-20.985	-24.015	27	-36	20.985	65.985	27
B_2B_3	0	-36	20.985	-65.985	9	36	20.985	24.015	9
B_3B_4	0	36	20.985	-65.985	81	18	-20.985	24.015	81
B_4B_0	0	18	-20.985	-24.015	63	0	20.985	65.985	63
A_0B_0	0	0	20.958	-60.985	45	-18	-20.985	24.015	45
A_1B_0	22.5	0	20.958	-60.985	45	-18	-20.985	24.015	45
$A_0B_2B_3$	0	-36	20.985	-65.985	9	36	20.985	24.015	9
$A_1B_2B_3$	22.5	-36	20.985	-65.985	9	36	20.985	24.015	9

TABLE III. Setting angles of HWPs for measurement devices. For any context, the angles of $H_{B_8, B_{11}, B_{14}, B_{18}, B_{21}}$, $H_{B_5, B_{13}, B_{20}}$, and H_{B_6} are fixed at 0° , 45° and 90° , respectively.

After the measurement of the observable B_j – whose results were mapped to two orthogonal polarizations –, the state of the system has to be transformed to the eigenstates of B_j before the sequential measurement of $B_{(j+1) \bmod 5}$ on the same photon [38]. The outcomes of B_j are each directed into identical but separated devices, i.e., H_{B_8, B_9} - BD_5 - $H_{B_{10}, B_{11}}$ for re-creating the eigenstate corresponding to the degenerated eigenvalues, while $H_{B_{16}}$ - BD_8 - $H_{B_{17}, B_{18}}$ for re-creating the eigenstate corresponding to the nondegenerated eigenvalue.

Then, two identical $B_{(j+1) \bmod 5}$ measuring devices (one is constructed by $H_{B_{12}}$ - $H_{B_{15}}$, BD_6 - BD_7 , and another by $H_{B_{19}}$ - $H_{B_{22}}$, BD_9 - BD_{10}) are built, each of which is connected to one of the output ports of the measuring device of B_j (each output port corresponds to either degenerated or non-degenerated eigenstate of B_j , respectively). The angles of the HWPs for Bob's measurements are listed in Table III. The joint probabilities of the outcomes, for each context, are estimated by coincidence count rates at detectors (D_{B_1} - D_{B_6}); the precise assignments of each double (or triple) of outcomes to detectors, for each measured context, are shown in Tables IV and V.

Observable	$p(-1, -1)$	$p(-1, 1)$	$p(1, -1)$	$p(1, 1)$
B_0B_1	$\sum_{m=1,2;n=4,5} C_{Am, Bn}$	$\sum_{m=1,2} C_{Am, B6}$	$\sum_{m=1,2;n=1,2} C_{Am, Bn}$	$\sum_{m=1,2} C_{Am, B3}$
B_1B_2	$\sum_{m=1,2} C_{Am, B1}$	$\sum_{m=1,2;n=2,3} C_{Am, Bn}$	$\sum_{m=1,2} C_{Am, B6}$	$\sum_{m=1,2;n=4,5} C_{Am, Bn}$
B_2B_3	$\sum_{m=1,2;n=4,5} C_{Am, Bn}$	$\sum_{m=1,2} C_{Am, B6}$	$\sum_{m=1,2;n=1,2} C_{Am, Bn}$	$\sum_{m=1,2} C_{Am, B3}$
B_3B_4	$\sum_{m=1,2} C_{Am, B1}$	$\sum_{m=1,2;n=2,3} C_{Am, Bn}$	$\sum_{m=1,2} C_{Am, B6}$	$\sum_{m=1,2;n=4,5} C_{Am, Bn}$
B_4B_0	$\sum_{m=1,2;n=4,5} C_{Am, Bn}$	$\sum_{m=1,2} C_{Am, B6}$	$\sum_{m=1,2;n=1,2} C_{Am, Bn}$	$\sum_{m=1,2} C_{Am, B3}$
A_0B_0	$\sum_{n=4,5,6} C_{A1, Bn}$	$\sum_{n=1,2,3} C_{A1, Bn}$	$\sum_{n=4,5,6} C_{A2, Bn}$	$\sum_{n=1,2,3} C_{A2, Bn}$
A_1B_0	$\sum_{n=4,5,6} C_{A1, Bn}$	$\sum_{n=1,2,3} C_{A1, Bn}$	$\sum_{n=4,5,6} C_{A2, Bn}$	$\sum_{n=1,2,3} C_{A2, Bn}$

TABLE IV. Each of the joint probabilities $p(B_j = \pm 1, B_{(j+1) \bmod 5} = \pm 1)$ ($j = 1, \dots, 5$), and $p(A_i = \pm 1, B_0 = \pm 1)$ ($i = 0, 1$) is estimated by the sum of the certain coincidence rates $C_{Am, Bn}$ of the APDs D_{Am} and D_{Bn} with $m = 1, 2$ and $n = 1, \dots, 6$, normalized by the total coincidences between the APDs of Alice and Bob.

For the photon detection, we only register the coincidence rates between the detectors (single-photon avalanche photodiodes with 3ns time window) of Alice and Bob. For each measurement, we record clicks for 2s, and the total coincidence counts are about 5500. To test the KCBS inequality, the correlators $\langle B_j B_{(j+1) \bmod 5} \rangle$ are constructed from the measured joint probabilities, $p(b, b' | j, (j+1) \bmod 5)$, according to Eq. (10) of the main text. Similarly, we can evaluate the value of α_{CHSH} for the CHSH inequality with the correlators $\langle A_i B_j \rangle$ and $\langle A_i B_j B_{j'} \rangle$, which are

Observable	$p(-1, -1, -1)$	$p(-1, -1, 1)$	$p(-1, 1, -1)$	$p(-1, 1, 1)$	$p(1, -1, -1)$	$p(1, -1, 1)$	$p(1, 1, -1)$	$p(1, 1, 1)$
$A_0B_2B_3$	$\sum_{n=4,5} C_{A1,Bn}$	$C_{A1,B6}$	$\sum_{n=1,2} C_{A1,Bn}$	$C_{A1,B3}$	$\sum_{n=4,5} C_{A2,Bn}$	$C_{A2,B6}$	$\sum_{n=1,2} C_{A2,Bn}$	$C_{A2,B3}$
$A_1B_2B_3$	$\sum_{n=4,5} C_{A1,Bn}$	$C_{A1,B6}$	$\sum_{n=1,2} C_{A1,Bn}$	$C_{A1,B3}$	$\sum_{n=4,5} C_{A2,Bn}$	$C_{A2,B6}$	$\sum_{n=1,2} C_{A2,Bn}$	$C_{A2,B3}$

TABLE V. Similarly, each of the joint probabilities $P(A_i = \pm 1, B_2 = \pm 1, B_3 = \pm 1)$ ($i = 0, 1$) is estimated by the sum of the certain coincidence rates C_{A_m, B_n} of the APDs D_{A_m} and D_{B_n} with $m = 1, 2$ and $n = 1, \dots, 6$, normalized by the total coincidences between the APDs of Alice and Bob.

constructed from the measured joint probabilities according to

$$\langle A_x B_y \rangle = p(a = b|x, y) - p(a \neq b|x, y), \quad (16a)$$

$$\langle A_x B_y B_{y'} \rangle = p(a = b \cdot b'|x, y, y') - p(a \neq b \cdot b'|x, y, y'). \quad (16b)$$

It is worth mentioning that in the test of the CHSH inequality (7) of the main text, photon loss opens up a detection efficiency loophole in our experiment. A fair-sampling assumption is then taken here, which assumes the events selected out by the photonic coincidence counts is an unbiased representation of the whole sample.

EXPERIMENTAL DATA

In this section, we present the observed values of all correlators that are relevant for the tests of the KCBS and CHSH inequalities. Each of the following Tables corresponds to a specific prepared state, discriminated in the caption.

Observable	Theoretical prediction	Experimental value	α_{CHSH} or β_{KCBS}
$\langle A_0 B_0 \rangle$	0.0904	0.0904(102)	
$\langle A_1 B_0 \rangle$	-0.0545	-0.0541(112)	1.1043(438)
$\langle A_0 B_2 B_3 \rangle$	0.6754	0.6679(108)	
$\langle A_1 B_2 B_3 \rangle$	-0.4075	-0.4001(116)	
$\langle B_0 B_1 \rangle$	0.7889	0.7828(104)	
$\langle B_1 B_2 \rangle$	0.7889	0.7817(109)	
$\langle B_2 B_3 \rangle$	0.7889	0.7801(104)	3.9069(518)
$\langle B_3 B_4 \rangle$	0.7889	0.7828(105)	
$\langle B_4 B_0 \rangle$	-0.7889	-0.7823(96)	

TABLE VI. Measured expectation values $\langle A_i B_j \rangle$, $\langle A_i B_2 B_3 \rangle$ and $\langle B_j B_{(j+1) \bmod 5} \rangle$ for the input state $|\Psi_1(\phi)\rangle$ with $\phi = 0$. The distance is $\sum_{j=1}^5 (p_j - p'_j)^2 = 0.000016 \pm 0.000082$.

Observable	Theoretical prediction	Experimental value	α_{CHSH} or β_{KCBS}
$\langle A_0 B_0 \rangle$	0.1631	0.1626(104)	
$\langle A_1 B_0 \rangle$	0.1210	0.1206(114)	1.4141(448)
$\langle A_0 B_2 B_3 \rangle$	0.6314	0.6251(112)	
$\langle A_1 B_2 B_3 \rangle$	-0.5138	-0.5058(118)	
$\langle B_0 B_1 \rangle$	0.7946	0.7859(106)	
$\langle B_1 B_2 \rangle$	0.7659	0.7584(98)	
$\langle B_2 B_3 \rangle$	0.7919	0.7829(106)	3.8728(514)
$\langle B_3 B_4 \rangle$	0.7659	0.7581(98)	
$\langle B_4 B_0 \rangle$	-0.7946	-0.7875(106)	

TABLE VII. Measured expectation values $\langle A_i B_j \rangle$, $\langle A_i B_2 B_3 \rangle$ and $\langle B_j B_{(j+1) \bmod 5} \rangle$ for the input state $|\Psi_2(\phi)\rangle$ with $\phi = 0.096$. The distance is $\sum_{j=1}^5 (p_j - p'_j)^2 = 0.000029 \pm 0.000106$.

Observable	Theoretical prediction	Experimental value	α_{CHSH} or β_{KCBS}
$\langle A_0 B_0 \rangle$	0.2334	0.2313(100)	
$\langle A_1 B_0 \rangle$	0.2906	0.2894(118)	
$\langle A_0 B_2 B_3 \rangle$	0.5906	0.5859(108)	1.7083(438)
$\langle A_1 B_2 B_3 \rangle$	-0.6122	-0.6018(112)	
$\langle B_0 B_1 \rangle$	0.8100	0.7936(101)	
$\langle B_1 B_2 \rangle$	0.7261	0.7197(103)	
$\langle B_2 B_3 \rangle$	0.7658	0.7577(102)	3.7826(510)
$\langle B_3 B_4 \rangle$	0.7261	0.7180(103)	
$\langle B_4 B_0 \rangle$	-0.8100	-0.7936(101)	

TABLE VIII. Measured expectation values $\langle A_i B_j \rangle$, $\langle A_i B_2 B_3 \rangle$ and $\langle B_j B_{(j+1) \bmod 5} \rangle$ for the input state $|\Psi_3(\phi)\rangle$ with $\phi = 0.192$. The distance is $\sum_{j=1}^5 (p_j - p'_j)^2 = 0.000461 \pm 0.000470$.

Observable	Theoretical prediction	Experimental value	α_{CHSH} or β_{KCBS}
$\langle A_0 B_0 \rangle$	0.2987	0.2958(107)	
$\langle A_1 B_0 \rangle$	0.4481	0.4453(111)	
$\langle A_0 B_2 B_3 \rangle$	0.5546	0.5512(115)	1.9813(450)
$\langle A_1 B_2 B_3 \rangle$	-0.6991	-0.6890(117)	
$\langle B_0 B_1 \rangle$	0.8076	0.8005(105)	
$\langle B_1 B_2 \rangle$	0.6710	0.6649(109)	
$\langle B_2 B_3 \rangle$	0.7117	0.7038(108)	3.6339(536)
$\langle B_3 B_4 \rangle$	0.6710	0.6653(109)	
$\langle B_4 B_0 \rangle$	-0.8076	-0.7994(105)	

TABLE IX. Measured expectation values $\langle A_i B_j \rangle$, $\langle A_i B_2 B_3 \rangle$ and $\langle B_j B_{(j+1) \bmod 5} \rangle$ for the input state $|\Psi_4(\phi)\rangle$ with $\phi = 0.288$. The distance is $\sum_{j=1}^5 (p_j - p'_j)^2 = 0.000020 \pm 0.000096$.

Observable	Theoretical prediction	Experimental value	α_{CHSH} or β_{KCBS}
$\langle A_0 B_0 \rangle$	0.3375	0.3332(106)	
$\langle A_1 B_0 \rangle$	0.5420	0.5367(107)	
$\langle A_0 B_2 B_3 \rangle$	0.5342	0.5304(115)	2.1382(442)
$\langle A_1 B_2 B_3 \rangle$	-0.7483	-0.7379(114)	
$\langle B_0 B_1 \rangle$	0.8120	0.8042(103)	
$\langle B_1 B_2 \rangle$	0.6275	0.6221(108)	
$\langle B_2 B_3 \rangle$	0.6617	0.6538(107)	3.5034(529)
$\langle B_3 B_4 \rangle$	0.6275	0.6195(108)	
$\langle B_4 B_0 \rangle$	-0.8120	-0.8038(103)	

TABLE X. Measured expectation values $\langle A_i B_j \rangle$, $\langle A_i B_2 B_3 \rangle$ and $\langle B_j B_{(j+1) \bmod 5} \rangle$ for the input state $|\Psi_5(\phi)\rangle$ with $\phi = 0.351$. The distance is $\sum_{j=1}^5 (p_j - p'_j)^2 = 0.000013 \pm 0.000079$.

Observable	Theoretical prediction	Experimental value	α_{CHSH} or β_{KCBS}
$\langle A_0 B_0 \rangle$	0.3763	0.3719(108)	
$\langle A_1 B_0 \rangle$	0.6355	0.6304(106)	2.2972(446)
$\langle A_0 B_2 B_3 \rangle$	0.5151	0.5112(117)	
$\langle A_1 B_2 B_3 \rangle$	-0.7946	-0.7837(115)	
$\langle B_0 B_1 \rangle$	0.8168	0.8079(103)	
$\langle B_1 B_2 \rangle$	0.5732	0.5691(109)	3.3397(446)
$\langle B_2 B_3 \rangle$	0.5940	0.5861(109)	
$\langle B_3 B_4 \rangle$	0.5732	0.5676(109)	
$\langle B_4 B_0 \rangle$	-0.8168	-0.8090(103)	

TABLE XI. Measured expectation values $\langle A_i B_j \rangle$, $\langle A_i B_2 B_3 \rangle$ and $\langle B_j B_{(j+1) \bmod 5} \rangle$ for the input state $|\Psi_6(\phi)\rangle$ with $\phi = 0.421$. The distance is $\sum_{j=1}^5 (p_j - p'_j)^2 = 0.000011 \pm 0.000071$.

Observable	Theoretical prediction	Experimental value	α_{CHSH} or β_{KCBS}
$\langle A_0 B_0 \rangle$	0.4078	0.4039(104)	
$\langle A_1 B_0 \rangle$	0.7116	0.7050(99)	2.4246(423)
$\langle A_0 B_2 B_3 \rangle$	0.5007	0.4975(112)	
$\langle A_1 B_2 B_3 \rangle$	-0.8294	-0.8182(108)	
$\langle B_0 B_1 \rangle$	0.8212	0.8127(97)	
$\langle B_1 B_2 \rangle$	0.5173	0.5104(104)	3.1580(506)
$\langle B_2 B_3 \rangle$	0.5194	0.5119(104)	
$\langle B_3 B_4 \rangle$	0.5173	0.5114(104)	
$\langle B_4 B_0 \rangle$	-0.8212	-0.8116(97)	

TABLE XII. Measured expectation values $\langle A_i B_j \rangle$, $\langle A_i B_2 B_3 \rangle$ and $\langle B_j B_{(j+1) \bmod 5} \rangle$ for the input state $|\Psi_7(\phi)\rangle$ with $\phi = 0.487$. The distance is $\sum_{j=1}^5 (p_j - p'_j)^2 = 0.000071 \pm 0.000172$.

Observable	Theoretical prediction	Experimental value	α_{CHSH} or β_{KCBS}
$\langle A_0 B_0 \rangle$	0.4340	0.4300(108)	
$\langle A_1 B_0 \rangle$	0.7746	0.7684(100)	2.5291(435)
$\langle A_0 B_2 B_3 \rangle$	0.4901	0.4885(116)	
$\langle A_1 B_2 B_3 \rangle$	-0.8549	-0.8422(111)	
$\langle B_0 B_1 \rangle$	0.8254	0.8198(99)	
$\langle B_1 B_2 \rangle$	0.4578	0.4518(107)	2.9684(519)
$\langle B_2 B_3 \rangle$	0.4359	0.4285(107)	
$\langle B_3 B_4 \rangle$	0.4578	0.4533(107)	
$\langle B_4 B_0 \rangle$	-0.8254	-0.8150(99)	

TABLE XIII. Measured expectation values $\langle A_i B_j \rangle$, $\langle A_i B_2 B_3 \rangle$ and $\langle B_j B_{(j+1) \bmod 5} \rangle$ for the input state $|\Psi_8(\phi)\rangle$ with $\phi = 0.553$. The distance is $\sum_{j=1}^5 (p_j - p'_j)^2 = 0.000012 \pm 0.000073$.

Observable	Theoretical prediction	Experimental value	α_{CHSH} or β_{KCBS}
$\langle A_0 B_0 \rangle$	0.4572	0.4515(113)	
$\langle A_1 B_0 \rangle$	0.8308	0.8228(102)	2.5714(451)
$\langle A_0 B_2 B_3 \rangle$	0.4828	0.4830(121)	
$\langle A_1 B_2 B_3 \rangle$	-0.8726	-0.8591(115)	
$\langle B_0 B_1 \rangle$	0.8299	0.8238(102)	
$\langle B_1 B_2 \rangle$	0.3841	0.3788(111)	2.7277(537)
$\langle B_2 B_3 \rangle$	0.3274	0.3228(111)	
$\langle B_3 B_4 \rangle$	0.3841	0.3803(111)	
$\langle B_4 B_0 \rangle$	-0.8299	-0.8220(102)	

TABLE XIV. Measured expectation values $\langle A_i B_j \rangle$, $\langle A_i B_2 B_3 \rangle$ and $\langle B_j B_{(j+1) \bmod 5} \rangle$ for the input state $|\Psi_9(\phi)\rangle$ with $\phi = 0.631$. The distance is $\sum_{j=1}^5 (p_j - p'_j)^2 = 0.000048 \pm 0.000148$.

Observable	Theoretical prediction	Experimental value	α_{CHSH} or β_{KCBS}
$\langle A_0 B_0 \rangle$	0.4657	0.4658(118)	
$\langle A_1 B_0 \rangle$	0.8594	0.8594(105)	2.6739(468)
$\langle A_0 B_2 B_3 \rangle$	0.4804	0.4805(126)	
$\langle A_1 B_2 B_3 \rangle$	-0.8682	-0.8682(119)	
$\langle B_0 B_1 \rangle$	0.8250	0.8250(105)	
$\langle B_1 B_2 \rangle$	0.3065	0.3065(115)	2.4726(555)
$\langle B_2 B_3 \rangle$	0.2121	0.2121(115)	
$\langle B_3 B_4 \rangle$	0.3056	0.3056(115)	
$\langle B_4 B_0 \rangle$	-0.8233	-0.8234(105)	

TABLE XV. Measured expectation values $\langle A_i B_j \rangle$, $\langle A_i B_2 B_3 \rangle$ and $\langle B_j B_{(j+1) \bmod 5} \rangle$ for the input state $|\Psi_{10}(\phi)\rangle$ with $\phi = 0.708$. The distance is $\sum_{j=1}^5 (p_j - p'_j)^2 = 0.000025 \pm 0.000100$.

Observable	Theoretical prediction	Experimental value	α_{CHSH} or β_{KCBS}
$\langle A_0 B_0 \rangle$	0.4771	0.4723(117)	
$\langle A_1 B_0 \rangle$	0.8787	0.8751(105)	2.6871(465)
$\langle A_0 B_2 B_3 \rangle$	0.4853	0.4831(125)	
$\langle A_1 B_2 B_3 \rangle$	-0.8665	-0.8566(118)	
$\langle B_0 B_1 \rangle$	0.8374	0.8306(105)	
$\langle B_1 B_2 \rangle$	0.2352	0.2280(115)	2.2065(553)
$\langle B_2 B_3 \rangle$	0.0927	0.0907(113)	
$\langle B_3 B_4 \rangle$	0.2352	0.2271(115)	
$\langle B_4 B_0 \rangle$	-0.8374	-0.8301(105)	

TABLE XVI. Measured expectation values $\langle A_i B_j \rangle$, $\langle A_i B_2 B_3 \rangle$ and $\langle B_j B_{(j+1) \bmod 5} \rangle$ for the input state $|\Psi_{11}(\phi)\rangle$ with $\phi = 0.785$. The distance is $\sum_{j=1}^5 (p_j - p'_j)^2 = 0.000025 \pm 0.000109$.